

The Stabilizing Role of the Intramolecular C–H···O Hydrogen Bond in Cyclic Amides Derived From α -Methylbenzylamine

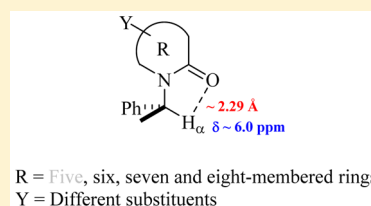
Jacinto Sandoval-Lira,[†] Lilia Fuentes,[†] Leticia Quintero,[†] Herbert Höpfl,[‡] Julio M. Hernández-Pérez,^{*,†} Joel L. Terán,^{*,†} and Fernando Sartillo-Piscil^{*,†}

[†]Centro de Investigación de la Facultad de Ciencias Químicas and Centro de Química de la Benemérita, Universidad Autónoma de Puebla, México. 14 Sur Esq. San Claudio, San Manuel, C. P. 72570, Puebla, México

[‡]Centro de Investigaciones Químicas, Universidad Autónoma del Estado de Morelos, Av. Universidad 1001, C. P. 62209, Cuernavaca, México

Supporting Information

ABSTRACT: A series of five-, six-, seven-, and eight-membered lactams containing the chiral auxiliary α -methylbenzylamine were structurally analyzed and further studied by DFT calculations with the purpose to examine with detail the previously detected intramolecular C–H···O hydrogen-bonding interaction formed between the hydrogen atom of the α -methylbenzylamine and the carbonyl group of the cyclic amide. The main objective was to establish whether its presence does have a tangible relevance in their spatial arrangement in solution and in the solid state or is a simple and not stabilizing interaction.



INTRODUCTION

In the past, there has been some controversy about the existence and importance of C–H···X (X = O, N, S, Hal) hydrogen-bonding interactions.¹ Today, after the seminal contributions of Desiraju^{2c–e} and Steiner,^{2a–c} it is now widely accepted that these contacts are relevant not only for the interpretation and understanding of the organization of molecular compounds in the solid state but also for the analysis of a widespread spectrum of additional phenomena in solution, particularly true for C–H···O contacts.³ For being a relative weak interaction with energies that generally did not exceed the 3 kcal/mol,⁴ it is frequently difficult to evidence with certainty that a given contact is indeed an attractive interaction. However, if the system under study is examined from varying perspectives such as spectroscopy data, X-ray diffraction analysis, and theoretical calculations, it is frequently possible to draw concise conclusions. Fundamental studies of Steiner^{2a} based on the systematic examination of a large number of single-crystal X-ray structures using the Cambridge Structural Database have shown that C–H···O contacts have a large probability to be attractive, if the H···O distances and the C–H···O angles are in the range of 2.2–2.4 Å and 90–130°, respectively. These values are reasonable, when considering that the carbon and oxygen atoms within the C–H···O triatomic sequence carry negative formal charges, while the intermediate hydrogen atom is positively polarized (C^{δ-}–H^{δ+}···O^{δ-}). Short H···O distances and small C–H···O angles would generate repulsive C^{δ-}···O^{δ-} electrostatic interactions that might involve even further substituents on the carbon and oxygen atoms.

In what follows, some representative examples are provided that highlight the relevance of analyzing with detail weak C–H···O hydrogen-bonding contacts for the understanding of particular phenomena on the molecular level. For instance, in

1997, Corey⁵ postulated that the presence of an intramolecular C–H···O hydrogen bond in the proposed three-component transition state **1** is responsible for the stereoselectivity in the enantioselective Diels–Alder reactions catalyzed by a chiral boron complex.

More recently, Scheiner and Smith⁶ demonstrated in a combined experimental and theoretical study of the pharmaceutically relevant α -fluoroamide **2** that an intramolecular C–H···O hydrogen-bonding interaction contributes significantly to the stabilization of the *cis*-planar conformer instead of the *trans*-planar stereoisomer that otherwise would be more stable (Figure 1).

In a similar scenario, our research group⁷ proposed that an intramolecular C–H···O hydrogen bond influences the conformational equilibrium of the chiral acetamide **3** (which

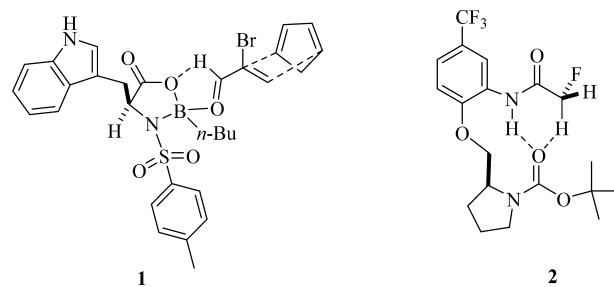
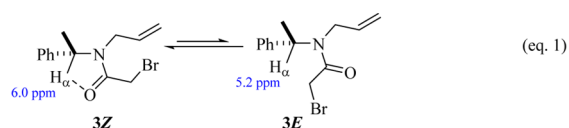


Figure 1. Representative examples showing the influence of C–H···O hydrogen-bonding interaction in chemical transformations (**1**) and conformational preferences (**2**).

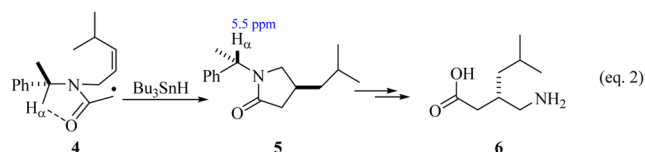
Received: February 13, 2015

Published: April 6, 2015

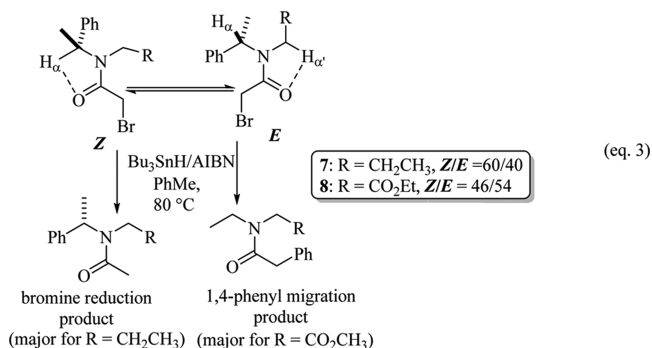
is derived from the well-known chiral auxiliary α -methylbenzylamine)⁸ and stabilizes the *Z*-rotamer. The C–H \cdots O interaction was postulated based on the deshielding effect of the carbonyl group on the C–H $_{\alpha}$ hydrogen in the ¹H NMR spectrum and further supported by theoretical calculations (eq 1). Meanwhile the chemical shift of H $_{\alpha}$ for the *Z*-rotamer is centered around 6 ppm, for the *E*-rotamer this hydrogen resonates at approximately 5.2 ppm.



In a subsequent publications,⁹ it was proposed that the C–H $_{\alpha}\cdots$ O interaction might be responsible for the stereoselectivity in the reaction of the α -amide radical **4** to form chiral pyrrolidones **5**, which are employed for the enantiopure synthesis of the biologically active γ -amino acid pregabalin **6** (eq 2).



Additionally, for a related system it was demonstrated that the *Z* \rightleftharpoons *E* conformational equilibrium can be shifted toward the otherwise less populated conformer by the suitable incorporation of another competitive and “stronger” intramolecular C–H \cdots O hydrogen-bond donor such as a hydrogen atom placed at the α position to a carbonyl group (H $_{\alpha}'$ in eq 3).¹⁰ This reverse conformational behavior provides an



important effect on the product distribution in the Stanyl radical reaction of α -bromoacetamides **7** and **8** (eq 3). For example, the chiral acetamide **7**, which exists in a major *Z*-conformation, gives preferentially the bromine reduction product; meanwhile acetamide **8**, showing major *E*-conformation, is prone to the ipso attack on the phenyl group, gives mainly the 1,4-phenyl radical migration product (eq 3).¹⁰

In spite of these experimental findings that support not only the existence of intramolecular C–H \cdots O hydrogen bonds in amides derived from α -methylbenzylamine on the conformational equilibria but also its role on molecular reactivity, we have not presented yet a conclusive systematic study of this compound class (which apart from NMR spectroscopic data) that provides strong additional support from either crystallographic analyses and/or theoretical calculations. In this context,

we present now a combined crystallographic and theoretical study of a series of representative cyclic amides derived from the chiral auxiliary α -methylbenzylamine that provide strong evidence in favor of the above-described proposals. Previously, in the context of a project directed toward the synthesis of chiral N-heterocycles derived from α -methylbenzylamine, we have reported a number of single-crystal X-ray structures of this type of cyclic amides, which provided the input for this research project and enabled us to perform the comprehensive study reported herein.

COMPUTATIONAL METHODS

Geometry optimizations were carried out using the B3LYP¹¹ density functional and 6-31G(d)¹² basis set. Minima were confirmed by vibrational analysis, which in all cases showed no imaginary frequencies. The energetic profiles for **9–13** and **15** include zero point energy (ZPE) and D3 dispersion corrections.^{13–15} ¹H Isotropic shielding values were calculated using the GIAO method at the B3LYP/6-31++G(2d,p)//B3LYP/6-31G(d) level of theory with the SDM model to describe the solvent effect. The CDCl₃ ($\epsilon = 4.7$) was considered as the solvent, and the values were scaled using the equation:

$$\delta_{\text{calcd}} = (b - \sigma_{\text{calcd}})/a$$

where a and b are -1.0591 and 31.6430 , respectively.¹⁶ Topological analysis of the electron density analysis for all studied structures uses the QTAIM methodology implemented in the AIMAll program.¹⁷ All calculations were performed with the Gaussian 09 software package,¹⁸ and the resulting structures were visualized with the Chemcraft 1.6 program.

RESULTS AND DISCUSSION

For the present study, the mainly premise was the following consideration: if the C–H $_{\alpha}\cdots$ O contact in the cyclic amides examined herein is attractive, then it must contribute to the stabilization of a molecular conformation, in which the lactam and the five-membered hydrogen-bonded (N)C–H $_{\alpha}\cdots$ O(C) ring are fused into a type of bicyclic rearrangement, as shown in Figure 2.

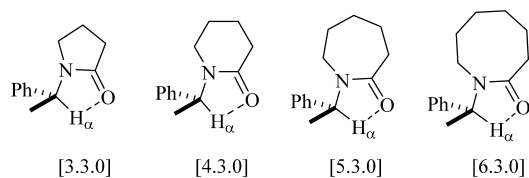


Figure 2. Bicycle-type molecular conformations formed at the expense of an attractive intramolecular C–H $_{\alpha}\cdots$ O hydrogen-bonding interaction in cyclic amides derived from α -methylbenzylamines.

The single-crystal X-ray diffraction structures examined herein were allowed to establish if the molecular structures of the corresponding cyclic amides exhibited reasonable geometrical parameters for attractive C–H \cdots O hydrogen-bonding interactions. Since it cannot be excluded that the geometrical parameters are casual, in the context of being a consequence of other relatively strong intra- and intermolecular interactions, theoretical calculations were performed on single molecules in the gas phase to prove otherwise and accomplish the solution-(NMR spectroscopy) and the solid-state analysis. To examine the reliability of the obtained geometries and to confirm the

existence of the C–H \cdots O hydrogen bond, an electron density analysis was accomplished using the quantum theory of atoms in molecules (QTAIM).¹⁹ For each bond critical point of interest, the electron density ρ_{BCP} and its Laplacian $\nabla^2\rho_{\text{BCP}}$ are reported.

Examination of the [3.3.0] System. The present research project was initiated with the theoretical study of pyrrolidine **9**⁷ as a representative example for a [3.3.0] bicycle-type conformation. Unfortunately for this cyclic amide, crystallographic data were not available. Nevertheless it was convenient to include this system for the purpose of comparison to larger cyclic amides, for which X-ray crystallographic information was available. According to the ¹H NMR spectrum of **9**, wherein the C–H α resonates at $\delta = 5.48$ ppm (recorded in CDCl₃), it can be inferred that an intramolecular C–H α \cdots O contact is absent. This is further proved by the calculated torsion energy profile, which was established by rotating the α -methylbenzyl group as a function of the C–N–C–H dihedral angle, hereinafter denoted as $\varphi(\text{CNCH})$. This profile was conducted through partial geometry optimization varying the dihedral angles in subsequent steps of 15°. For the global minima, additionally an unconstrained optimization was performed, which allowed to establish the $\varphi(\text{CNCH})$ with precision. This analysis provided two minima at $\varphi(\text{CNCH}) = 1.4^\circ$ (conformer **9a**) and 164° (conformer **9b**) with an energy difference of 1.2 kcal/mol. In the more energetic conformer **9b**, the H α and O atoms have almost antiparallel orientation (Figure 3). On the

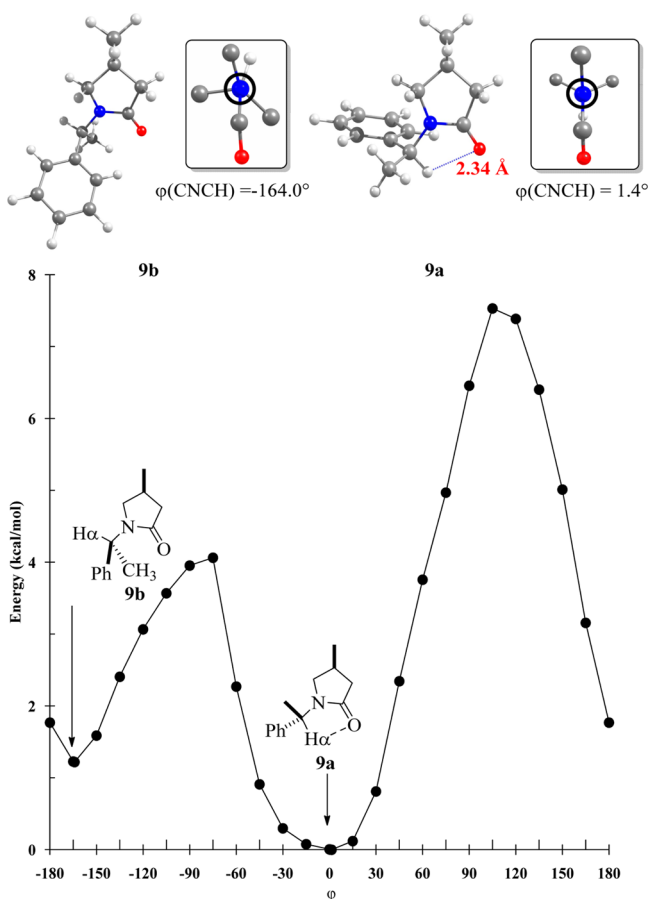


Figure 3. Rotational energy profile of pyrrolidinone **9**⁷ with illustration of the optimized structures corresponding to the energy minima (with Newman projection).

contrary, for rotamer **9a**, these atoms are eclipsed with a H \cdots O distance of 2.34 Å and an H \cdots O angle of 108.1°, both of which are within the range of established for attractive C–H \cdots O interactions.^{2e} Although at first glance, this geometry appears to be in favor of an attractive C–H α \cdots O interaction, the electron density analysis for **9a** does not exhibit a bond critical point between the H α and O atoms (see Figure S3 in Supporting Information), indicating that albeit the geometric parameters are within the established limits for such contacts, both atoms are apparently not interacting in an attractive way.

In addition, the calculated chemical shift of H α for **9a** at 5.46 ppm is in excellent agreement with the experimental value (5.48 ppm) and confirms the absence of an attractive C–H α \cdots O interaction. This outlier from what is expected might be attributed to a lower sp²-bond character of the C–N amide bond²⁰ within the five-membered lactam ring, which introduces bond angle strain that might alternate the electron density distribution within the amide group and thus makes less effective the electron donation toward the hydrogen acceptor.

Examination of the [4.3.0] System. For compounds with [4.3.0] bicycle-type molecular conformation, a larger number of experimentally determined structures was available, i.e., piperidones **10**,²¹ **11**,²² **12**,²³ and **13**,²⁴ which were modeled by theoretical calculations. The rotational profile of **10** gave two minima (**10a** and **10b**) with an energy difference of 3.5 kcal/mol and a rotational energy barrier of 6.4 kcal/mol (Figure 4). These energy values are considerably higher than those observed for pyrrolidine **9** and hence indicate that the population of **10a** should be significantly larger than that of rotamer **10b**. In the conformation corresponding to the local minimum found for **10b**, the C–H α bond is almost anti-periplanar to the carbonyl group [$\varphi(\text{CNCH}) = 162.1^\circ$], while the phenyl and methyl substituents are close to the C=O oxygen. On the contrary, in the molecular structure of **10a**, the conformation is syn-parallel [$\varphi(\text{CNCH}) = 1.4^\circ$], with a H α \cdots O distance of 2.21 Å and a H α \cdots O bond angle of 109.8°. When compared to conformers **9a/9b**, we found that the **10a/10b** energy difference is larger ($\Delta E = 1.2$ and 3.5 kcal/mol, respectively), and the energy barrier for the rotation barrier is also higher ($\Delta E = 4.1$ and 6.4 kcal/mol, respectively), which is in agreement with an attractive C–H α \cdots O interaction, as suggested also by the chemical shift of H α centered at 5.91 ppm (recorded in CDCl₃), which is very close to the computed value (6.1 ppm). Interestingly, the single-crystal X-ray data of **10a** are in agreement with the computed data: The H α and the C=O oxygen atoms are eclipsed with an interatomic distance of 2.31 Å that is considerably shorter than the sum of their van der Waals radii (2.72 Å) (Figure 5). Also, the experimental C–H α \cdots O bond angle of 107.5° is also in close concordance with the computed value (109.8°).

Further and conclusive experimental evidence for the presence of an attractive C–H α \cdots O interaction was provided by the analysis of the electron density calculated for rotamer **10a**, which presented a bond critical point between H α and O with density and Laplacian values of 0.0204 and 0.0796 au, respectively (see Figure S4 in Supporting Information). These values are within the established parameters of a weak hydrogen bond with electrostatic/disperse character.²⁵ Therefore, it is supported that piperidone **10** exists preferentially comfortable in a [4.3.0] bicycle-type structure, which corresponds to the Z-conformation, both in solution and the solid state, and that the C–H α \cdots O contact is responsible for this conformational preference.

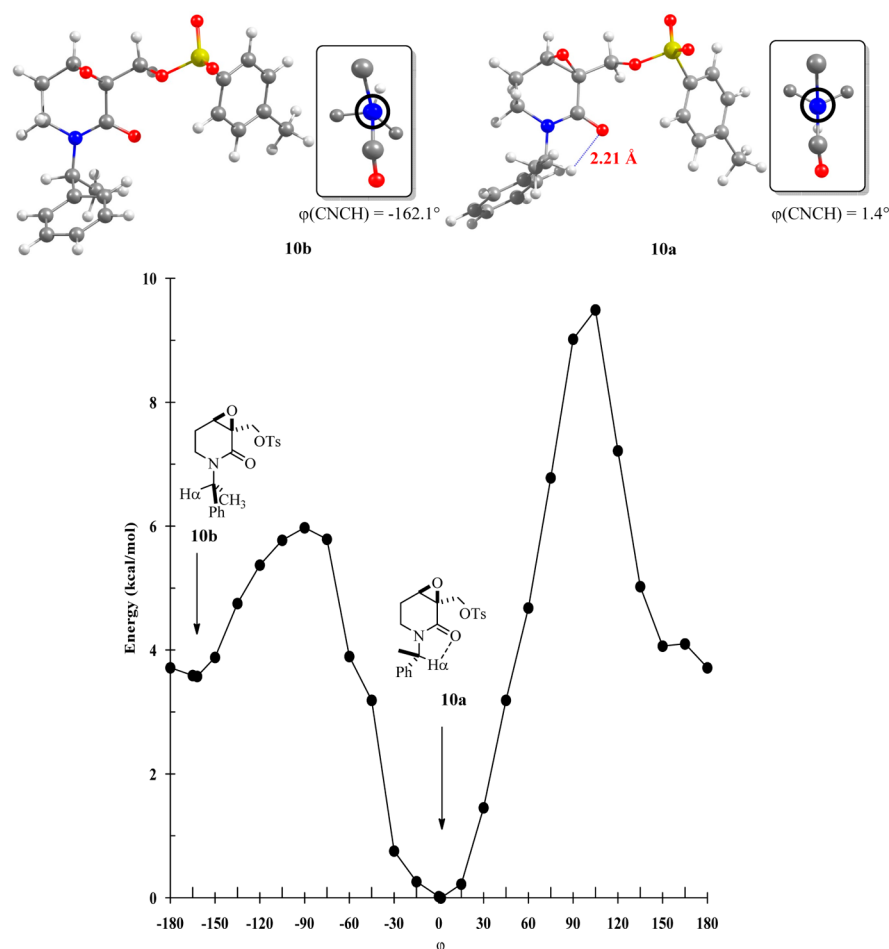


Figure 4. Rotational profile of piperidone 10. Minima optimized structures are illustrated (with Newman projection).

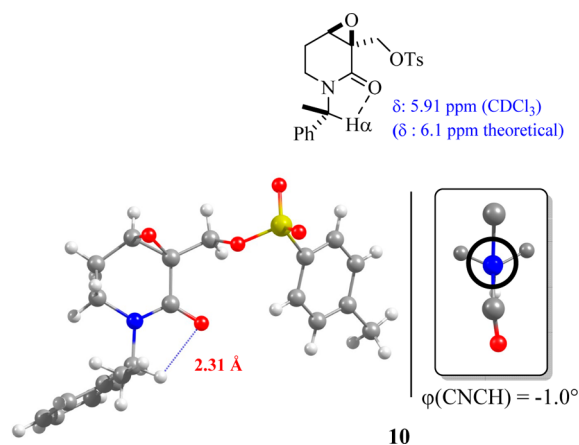


Figure 5. Single-crystal X-ray structure and ^1H NMR shift for the H_α of piperidone 10.²¹

Despite the molecular structures of piperidones 11,²² 12,²³ and 13²⁴ are quite different from piperidone 10, their crystallographic information regarding the $\text{H}_\alpha\cdots\text{O}$ contact, the ^1H NMR (in CDCl_3) data, and the computed chemical shifts are very similar. As for 10, the chemical shifts for H_α in 11–13 are centered close to 6.0 ppm (Figure 6).

The rotational profiles of 11–13 exhibited a very similar behavior to that observed for piperidone 10. Two local minima were observed for molecular conformations with *anti*-parallel

$\text{C}-\text{H}_\alpha$ and $\text{C}=\text{O}$ bonds (11b–13b), and when $\text{C}-\text{H}_\alpha$ and $\text{C}=\text{O}$ bonds are *syn*-parallel (11a, 12a, and 13a), with the latter being more stable. The conformations corresponding to the global minima of 11a–13a have almost the same spatial arrangement as found in the corresponding X-ray structures, and for all cases the electron density analysis revealed bond critical points for the $\text{C}-\text{H}_\alpha\cdots\text{O}$ contacts (Table 1, entries 4 and 5, and also see Figures S5–S7 in Supporting Information). The most relevant geometrical parameters are summarized in Table 1 (entries 1–3). These are important finding, since it may be argued that intermolecular contacts and packing interactions in the solid-state structures might not be responsible for the preference of these molecular conformations. It is also important to remark that the presence of substituents at the C6 position in piperidones 11 and 13 apparently does not destabilize the conformations of 11a and 13a by steric congestion. This further supports that the $\text{C}-\text{H}_\alpha\cdots\text{O}$ contact should not be considered as either casual or accidental but as a relevant stabilizing factor that contributes to the stabilization of the [4.3.0] bicycle-type molecular conformation.

Examination of the [5.3.0] System. As example for [5.3.0] bicycle-type structure, we investigated 1,4-oxazepan-5-one 14.²⁶ This is an interesting case because the hydroxyl group at the C-6 position is capable of competing with the $\text{C}-\text{H}_\alpha\cdots\text{O}$ hydrogen-bonding interaction and because this compound crystallized with three crystallographically independent molecules within the same asymmetric unit (14a–14c) (Figure 7). Nevertheless, while in the three structures 14a–14c the $\text{C}-$

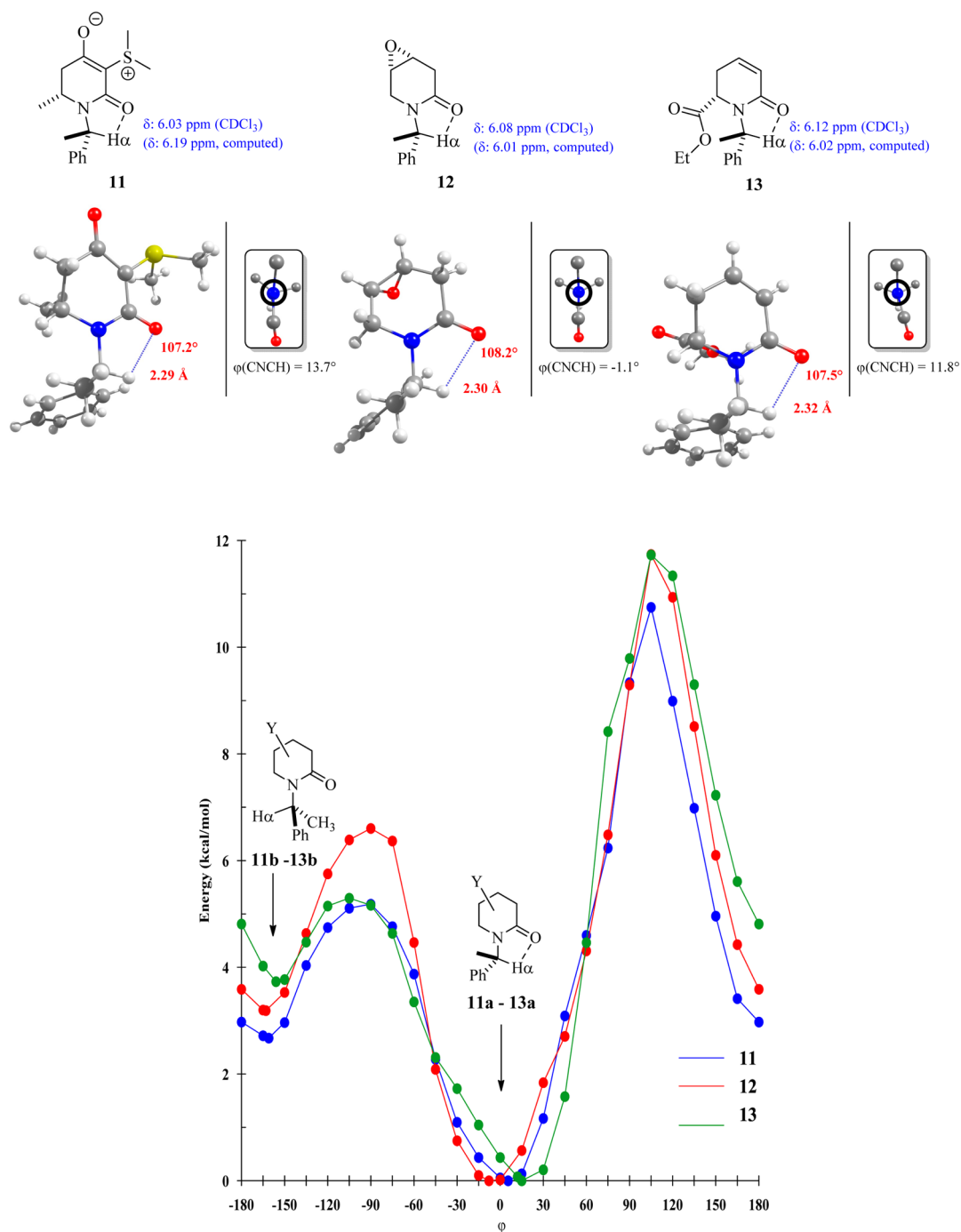


Figure 6. Single-crystal X-ray structures, ^1H NMR shifts for the C– H_α hydrogen atoms, and rotational energy profiles of piperidones 11,²² 12,²³ and 13²⁴ (with Newman projection).

Table 1. Calculated Parameters for the Geometry-Optimized Structures 11a–13a

entry	parameter	11a	12a	13a
1	$\text{H}_\alpha\cdots\text{O}$, Å	2.16	2.17	2.20
2	$\text{C}-\text{H}_\alpha\cdots\text{O}$, °	110.7	110.1	109.7
3	$\phi(\text{CNCH})$, °	5.5	-7.8	11.9
4	ρ_{BCP} , au	0.0219	0.0219	0.0204
5	$\nabla^2\rho_{\text{BCP}}$, au	0.0825	0.0830	0.0798

$\text{H}_\alpha\cdots\text{O}$ contact is clearly exhibited (14a, $\text{H}_\alpha\cdots\text{O} = 2.29 \text{ \AA}$, $\text{C}-\text{H}_\alpha\cdots\text{O} = 109.0^\circ$; 14b, $\text{H}_\alpha\cdots\text{O} = 2.29 \text{ \AA}$, $\text{C}-\text{H}_\alpha\cdots\text{O} = 109.4^\circ$; 14c, $\text{H}_\alpha\cdots\text{O} = 2.28 \text{ \AA}$, $\text{C}-\text{H}_\alpha\cdots\text{O} = 109.1^\circ$), the apparently

stronger $\text{OH}\cdots\text{O}$ hydrogen bond is retained in only two of the three structures (14a and 14b). In 14c, the OH group participates in an intermolecular $\text{O}-\text{H}\cdots\text{Cl}$ hydrogen bond. According to the reported ^1H NMR, chemical shift for H_α is centered at 6.15 ppm (CDCl_3), again, very close to the calculated value of 14a (6.03 ppm).

Single-point calculations on the molecular structures of 14a–14c showed that conformer 14a is the most stable ($\Delta E = 2.5 \text{ kcal/mol}$ for 14b and 6.7 kcal/mol for 14c), which is expected because of the stronger $\text{O}-\text{H}\cdots\text{O}$ hydrogen-bonding interaction ($\text{H}\cdots\text{O} = 2.06 \text{ \AA}$, $\text{O}-\text{H}\cdots\text{O} = 102.5^\circ$, and $\phi(\text{CCOH}) = 0.4^\circ$). In 14b, the $\text{O}-\text{H}\cdots\text{O}$ hydrogen bond is weakened by an

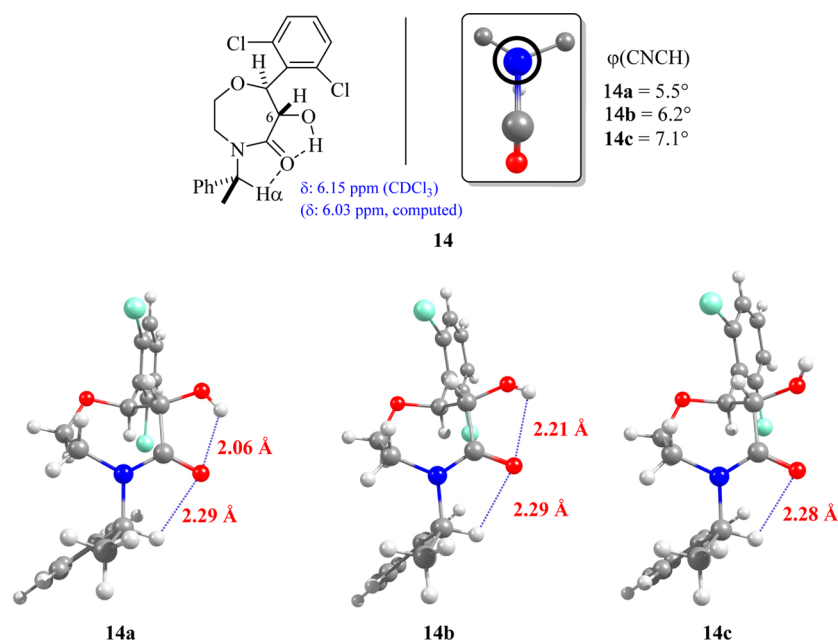


Figure 7. Single-crystal X-ray structures and ^1H NMR shift for the $\text{C}-\text{H}_\alpha$ hydrogen of 1,4-oxazepan-5-one **14**²⁶ (with Newman projection).

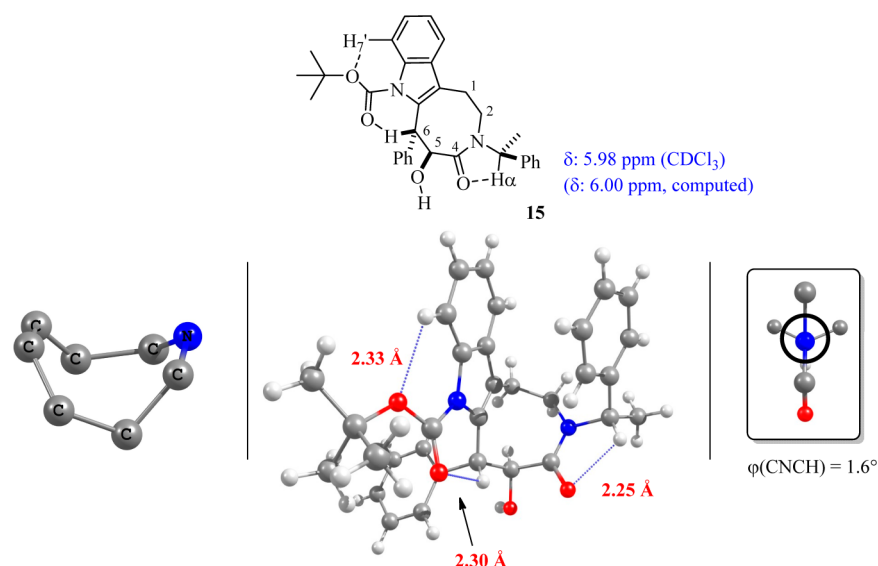


Figure 8. Single-crystal X-ray structure and ^1H NMR shift for the H_α of chiral lactam **15**^{27b} (with Newman projection).

increase of the $\text{H}\cdots\text{O}$ distance (2.21 Å) and a significant distortion of the $\varphi(\text{CCOH})$ dihedral angle from planarity (-34.0°), which also increases the $\text{O}-\text{H}\cdots\text{O}$ angle (105.8°). The loss of the $\text{O}-\text{H}\cdots\text{O}$ bond in **14c** ($\varphi(\text{CCOH}) = -110.3^\circ$) raises the relative energy to 6.7 kcal/mol. Despite being significantly weaker, it is interesting to find that all molecules **14a–14c** preserved the $\text{H}_\alpha\cdots\text{O}$ interaction and, moreover, with only slight changes in the geometric parameters ($\text{H}\cdots\text{O} = 2.28\text{--}2.29$ Å, $\text{C}-\text{H}\cdots\text{O} = 109^\circ$, and $\varphi(\text{CNCO}) = 6.2^\circ$). Additionally, the QTAIM analysis of **14a** revealed a bond critical point between H_α and $\text{O}=\text{C}$ with a density of 0.0202 and a Laplacian of 0.0810 au (see Figure S8 in Supporting Information).

Examination of the [6.3.0] System. The chiral eight-membered lactams derived from the indole derivatives **15**²⁷ and **16**²⁷ are further remarkably examples that permitted to put in context not only the presence of the $\text{C}-\text{H}\cdots\text{O}$ hydrogen-

bonding interaction in amides derived from the chiral auxiliary α -methylbenzylamine but also the relevance of this interaction in the conformational preference of the title compounds. It is worth mentioning that this [6.3.0] bicyclic systems represent an unconstrained system which enables $Z \rightleftharpoons E$ rotamer equilibrium similar to the acyclic rotamer systems.²⁸ Moreover, lactam **15** shows a single set of NMR signals, featuring the chemical shift of H_α at 5.98 ppm (CDCl_3), which indicates the presence of the single Z -rotamer, just as in the above-studied bicyclic systems. The X-ray crystallographic analysis of lactam **15** reveals not only the presence of the $\text{C}-\text{H}_\alpha\cdots\text{O}$ hydrogen bond but also two additional $\text{C}-\text{H}\cdots\text{O}$ contacts and the absence of the $\text{O}-\text{H}\cdots\text{O}$ hydrogen bond that should exist between the hydroxyl group at C5 and the amide carbonyl at C4 (Figure 8).^{27b}

It seems likely that these two additional $\text{C}-\text{H}\cdots\text{O}$ interactions are responsible not only for the observation of a

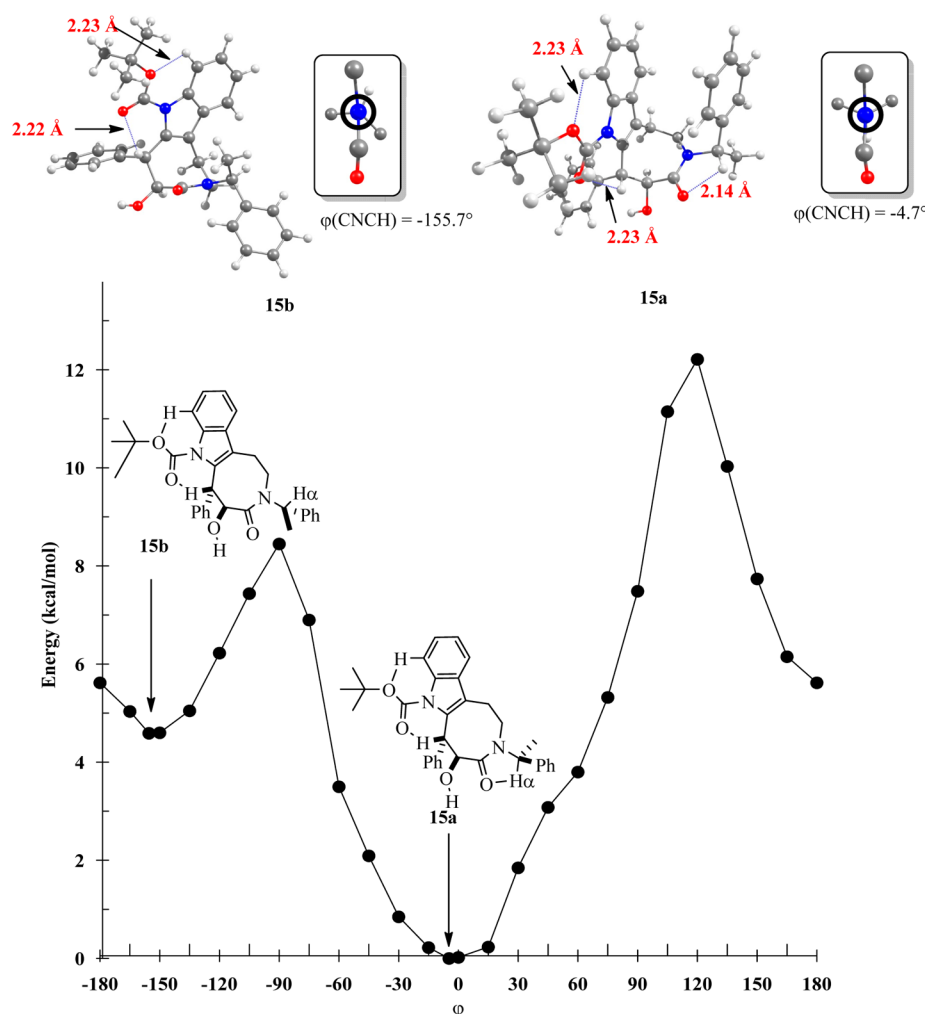


Figure 9. Rotational energy profile of the *N*-Boc protected lactam **15** with illustration of the optimized structures corresponding to the energy minima (with Newman projection).

single conformer either in solution (in CDCl_3) and the solid state but also for the preferential twist-boat conformation over the chair conformation, even though the latter has been proposed to be the lowest energy conformer.²⁹

The $\text{C}-\text{H}_\alpha\cdots\text{O}$ contact has a distance of 2.25 Å and a torsional angle $\varphi(\text{CNCH})$ of 1.6°. The additional $\text{C}-\text{H}\cdots\text{O}$ contacts, which are formed at expense of the BOC (*tert*-butyloxycarbonyl) protecting group, show crystallographic data consistent with the presence of a weak hydrogen-bonding interaction: $\text{H6}\cdots\text{O} = 2.30$ Å, and $\text{C}-\text{H6}\cdots\text{O} = 102^\circ$, $\text{H7}'\cdots\text{O} = 2.33$ Å, and $\text{C}-\text{H7}'\cdots\text{O} = 109.1$ Å.

As in the previous cases, the rotational energy profile of **15** showed two minima (**15a** and **15b**), with an energy barrier of 8.4 kcal/mol, which is approximately 2 kcal/mol higher than those observed for piperidones **10**–**13** (Figure 9). For the conformations corresponding to these minima, the $\text{H}\cdots\text{O}$ hydrogen contact with BOC was also confirmed. For **15b**, the calculated geometry data are in agreement with the crystallographic data ($\text{H7}'\cdots\text{O} = 2.23$ Å, $\text{C}-\text{H7}'\cdots\text{O} = 110.8^\circ$, $\rho_{\text{BCP}} = 0.0179$ au, and $\nabla^2\rho_{\text{BCP}} = 0.0677$ au; $\text{H6}\cdots\text{O} = 2.22$ Å, $\text{C}-\text{H6}\cdots\text{O} = 108.9^\circ$, $\rho_{\text{BCP}} = 0.0189$ au, and $\nabla^2\rho_{\text{BCP}} = 0.0726$ au). In the same vein, the corresponding descriptors for **15a** support the presence of the expected $\text{H}_\alpha\cdots\text{O}$ hydrogen bond ($\text{H}_\alpha\cdots\text{O} = 2.14$ Å, $\text{C}-\text{H}_\alpha\cdots\text{O} = 111.3^\circ$, $\varphi(\text{CNCH}) = -4.7^\circ$, $\rho_{\text{BCP}} = 0.0230$ au, and $\nabla^2\rho_{\text{BCP}} = 0.0871$ au) and the two additional $\text{C}-\text{H}\cdots\text{O}$

contacts ($\text{H7}'\cdots\text{O} = 2.23$ Å, $\text{C}-\text{H7}'\cdots\text{O} = 110.0^\circ$, $\rho_{\text{BCP}} = 0.0178$ au and $\nabla^2\rho_{\text{BCP}} = 0.0683$ au; $\text{H6}\cdots\text{O} = 2.23$ Å, $\text{C}-\text{H6}\cdots\text{O} = 108.6^\circ$, $\rho_{\text{BCP}} = 0.0189$ au and $\nabla^2\rho_{\text{BCP}} = 0.0728$ au) (see Figure S9 in Supporting Information).

Although lactam **16**,²⁷ in which the BOC protecting group was removed, did not afford suitable crystals for single-crystal X-ray diffraction studies, the NMR spectroscopy data and the theoretical calculations revealed important results to accomplish this research. The ^1H NMR spectrum of **16** reveals two sets of well-resolved signals, indicating the presence of a slow dynamic process between two species in a 54/46 ratio.²⁸ At first glance, the existence of a $Z \rightleftharpoons E$ rotamer equilibrium, similar to the acyclic systems, was considered (Figure 10). However, the chemical shifts of the signals for the $\text{C}-\text{H}_\alpha$ hydrogens are both centered at 5.94 and 5.88 ppm, which suggests that both molecular conformers exhibit $\text{H}_\alpha\cdots\text{O}$ hydrogen bonding and excludes the presence of an *E*-rotamer.

Based on conformational study of similar eight-membered lactams, in which an accessible chair \rightleftharpoons twist-boat equilibrium rather than a $Z \rightleftharpoons E$ rotamer interconversion was established,²⁹ we searched for possible conformations of the eight-membered lactam **16**. Two minima were found which exhibit a chair (**16a**) and a boat-twist conformation (**16b**). In agreement with the ^1H NMR data, both conformations featured a $\text{C}-\text{H}_\alpha\cdots\text{O}$ contact (Figure 11).

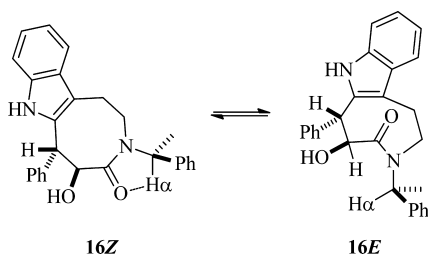


Figure 10. Expected *Z/E* interconversion for the eight-membered lactam **16**.

The energy difference between **16a** and **16b** is 3.25 kcal/mol, being **16a** the lowest energy conformer, which can be attributed to the presence of the additional O–H⋯O hydrogen bond ($H\cdots O = 1.92 \text{ \AA}$, $O-H\cdots O = 120.4^\circ$, and $\varphi(\text{HOC}(=\text{O})\text{O}) = 5.6^\circ$). The calculated ^1H NMR shifts for H_α in **16a** and **16b** are 6.20 and 6.02 ppm, respectively, which are in acceptable concordance with the experimental values: 5.87 and 5.94 ppm, respectively. The calculated $H_\alpha\cdots O$ distances for **16a** and **16b** (2.18 and 2.17 Å, respectively) are among the shortest distances found in this comparative study. The values for $\varphi(\text{CNCH})$ are -18.4° in **16a** and -8.7° in **16b**, and the $C_\alpha-H\cdots O$ angles are 107.7° for **16a** and 110.3° for **16b**. The QTAIM analysis established that the $C_\alpha-H\cdots O$ and $O-H\cdots O$ interactions in **16a** and **16b** are attractive (**16a**, $\rho_{\text{BCP}} = 0.0217 \text{ au}$, $\nabla^2\rho_{\text{BCP}} = 0.0829 \text{ au}$, and $\rho_{\text{BCP}} = 0.0217 \text{ au}$, $\nabla^2\rho_{\text{BCP}} = 0.0829 \text{ au}$; **16b**, $\rho_{\text{BCP}} = 0.0227 \text{ au}$, $\nabla^2\rho_{\text{BCP}} = 0.0905 \text{ au}$) (see Figures S10 and S11 in Supporting Information).

These combined experimental and theoretical observations regarding the **16a** \rightleftharpoons **16b** equilibrium indicate that the presence of the two $C-H\cdots O$ interactions in **15** is not only responsible for the presence of a single conformer but also for the absence of the chair conformational preference, which is preferentially observed in eight-membered lactams.²⁹

Analysis of the $C-H_\alpha$ Stretching. It has been established that a classical $X-H\cdots Y$ hydrogen-bonding interaction manifests a $X-H$ bond lengthening, which results in a red shift of the fundamental $X-H$ stretching, and it can be

observed in the IR spectra.^{2c} Interestingly, an inverse behavior is observed for the nonclassical $C-H\cdots Y$ hydrogen-bonding interactions (“improper” or “blue-shifted” hydrogen bonds) which present a $C-H$ bond shortening, and a blue shift of the IR stretching frequency is observed.³⁰ In this sense, an additional evidence of the presence of an $C-H_\alpha\cdots O$ interaction in cyclic amides derived from the chiral auxiliary α -methylbenzylamine can be obtained from the IR frequencies of the fundamental $C-H_\alpha$ stretching for all minima optimized structures. In order to quantify the percentage of shifting ($\% \Delta\nu$) of the $C-H_\alpha$ stretching when is bonded, eq 4 is used, wherein $\nu_{(C-H)\text{a}}$ corresponds to stretching frequency for conformers **a**, in which the $C-H_\alpha\cdots O$ contact is present; and $\nu_{(C-H)\text{b}}$ corresponds to conformers **b**, in which the $C-H_\alpha\cdots O$ contact is absent.

$$\% \Delta\nu = \frac{\nu_{(C-H)\text{a}} - \nu_{(C-H)\text{b}}}{\nu_{(C-H)\text{b}}} \times 100 \quad (4)$$

The frequencies of fundamental $C-H_\alpha$ stretching, distances, and relative infrared shifts are listed in Table 2. As we

Table 2. Calculated Frequencies of Fundamental $C-H_\alpha$ Stretching, Distances, and Relative Infrared Shifts

compound	conformers a		conformers b		%Δν
	distance (Å)	ν (cm ⁻¹)	distance (Å)	ν (cm ⁻¹)	
9	1.095	3083.17	1.097	3041.39	1.4
10	1.092	3111.87	1.095	3054.60	1.9
11	1.092	3124.53	1.095	3067.71	1.9
12	1.094	3124.72	1.096	3065.30	1.9
13	1.091	3132.07	1.095	3071.27	2.0
14	1.092	3114.86	–	–	–
15	1.092	3109.44	1.095	3055.37	1.8
16	1.091	3114.82	–	–	–

anticipated, shortening of $C-H_\alpha$ bond distance and a blue-shift are observed for conformers **a** (when $C-H_\alpha\cdots O$ contact is present). Interestingly, for compound **9**, in which the electron density analysis did not exhibit bond critical point between the

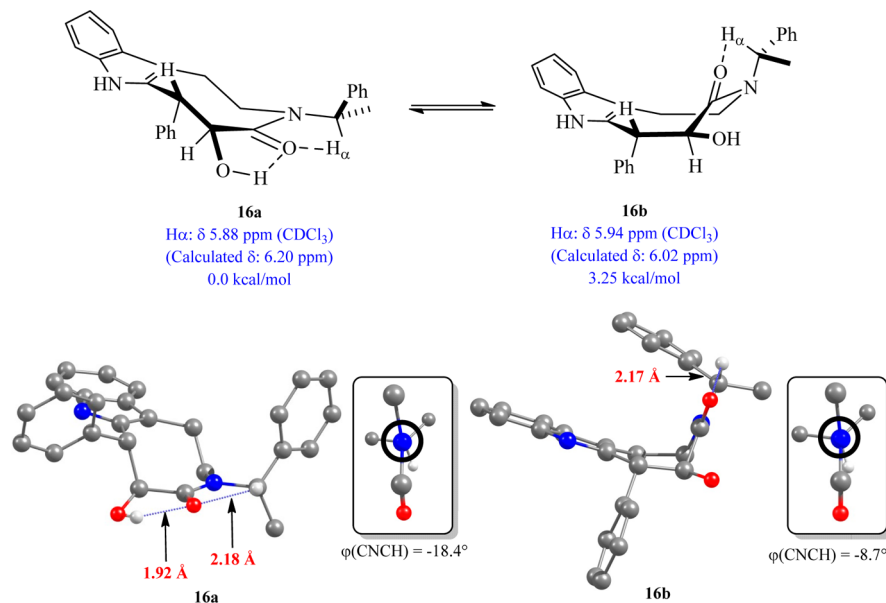


Figure 11. Geometry optimized structures and ^1H NMR data of the chair \rightleftharpoons boat-twist equilibrium for **16** (with Newman projection).

H_α and O atoms for **9a** (see Supporting Information), the lowest percentage of $\Delta\nu$ (1.4%) is observed. In the other cases, the $\% \Delta\nu$ is higher (~ 2), indicating that the C– H_α stretching for conformers a are more “blue-shifted”, which is in concordance with the presence of a weak C–H \cdots O hydrogen bonding.

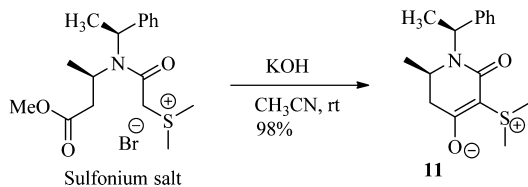
CONCLUSIONS

The combined crystallographic and theoretical study of selected cyclic amides derived from the chiral auxiliary α -methylbenzylamine evidenced that C–H \cdots O interactions influence significantly their molecular conformation in solution and the solid state. This study also demonstrated that the geometrical parameters alone are not sufficient to establish conclusively the existence of an attractive C–H \cdots O hydrogen-bonding interaction, so that additional experimental and theoretical data are required such as ^1H NMR spectroscopy and the quantum theory of atoms in molecules (QTAIM), which provides the electron density ρ_{BCP} and its Laplacian $\nabla^2\rho_{\text{BCP}}$ at the hydrogen bond critical point. Additionally, the analysis of the C– H_α stretching frequencies showed a shortening bond and a “blue-shifted” hydrogen bond in conformations where the C– $H_\alpha\cdots$ O interactions are present. This study affirms that the previously established empirical criterion for assigning the molecular geometries of *Z/E*-rotamers based on the chemical shift of H_α (approximately 6 ppm for the *Z*-rotamer and 5.2 ppm for the *E*-rotamer) is adequate and can, therefore, be recognized as an element for determining the stereochemistry of both cyclic and acyclic chiral amides derived from α -methylbenzylamine. Although this criterion could be interpreted as a simple anisotropic deshielding effect of the carbonyl group toward the H_α atom,³¹ our findings clearly demonstrated that albeit this might be true, the nature of this C–H \cdots O interaction is mainly responsible not only for the chemical shift of H_α at 6 ppm but also for the conformational preference of the cyclic amides derived from the chiral auxiliary α -methylbenzylamine.

EXPERIMENTAL SECTION

Reagents were obtained from commercial sources and used without purification. Solvents were used as technical grade and freshly distilled prior to use. NMR spectra were carried out with 400 and 300 MHz equipment. Internal references (TMS) for ^1H and ^{13}C chemical shifts are stated in parts per million.

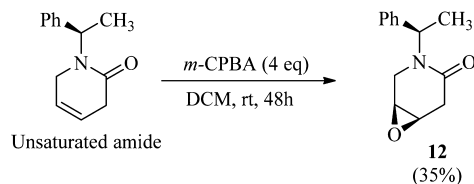
Compound **11** was prepared following the methodology previously reported.³²



(R)-5-(Dimethylsulfonio)-2-methyl-6-oxo-1-((S)-1-phenylethyl)-1,2,3,6-tetrahydropyridin-4-olate. To a stirred room temperature solution of the corresponding sulfonium salt (0.55 g, 1.36 mmol) in CH_3CN (28 mL) was added KOH (0.155 g, 2.7 mmol). After 12 h, the resulting mixture was filtered and dried under reduced pressure to give 0.38 g (98%) of the corresponding zwitterionic compound **11** as a white solid. Mp = 200–202 °C. $[\alpha]_{\text{D}}^{20} = -74.8$ (c 1.0, CH_2Cl_2). ^1H NMR (400 MHz, CDCl_3), δ 0.57 (d, $J = 6.4$ Hz, 3H), 1.54 (d, $J = 7.2$ Hz, 3H), 2.09 (dd, $J = 6.4, 15.0$ Hz, 1H), 2.69 (dd, $J = 6.4, 15.0$ Hz, 1H), 2.94 (s, 3H), 3.02 (s, 3H), 3.58 (m, 1H), 6.01 (q, $J = 7.2$ Hz, 1H), 7.23–7.44 (m, 5H). ^{13}C NMR (100 MHz, CDCl_3) δ 16.8, 18.7,

26.0, 27.7, 44.5, 44.6, 49.5, 73.2, 127.3, 128.1, 128.2, 141.2, 164.8, 187.1.

(1S,6R)-3-((R)-1-Phenylethyl)-7-oxa-3-azabicyclo[4.1.0]-heptan-4-one (12). To a stirred room temperature solution of the



corresponding unsaturated amide (0.6 g, 3.0 mmol) in CH_2Cl_2 (7 mL) was added *m*CPBA (0.35 g, 1.56 mmol, 77% purity). After 48h, the reaction was quenched by addition of a solution of NaHCO_3 (3 mL, 10% aqueous solution), following addition of a brine solution. The organic phase was separated and dried over anhydrous Na_2SO_4 and filtered, and the solvent was evaporated. The resulting mixture was purified through column chromatography (1:2, ethyl acetate/petroleum ether, respectively, on SiO_2) afforded 0.22 g (35%) of the desired 2,4-epoxyamide **12** as a white solid. Mp = 109 °C. $[\alpha]_{\text{D}}^{20} = -101.3$ (c 1.0, CH_2Cl_2). ^1H NMR (400 MHz, CDCl_3), δ 1.51 (d, $J = 7.2$ Hz, 3H), 2.82 (dd, $J = 1.55, 18.3$ Hz, 1H), 3.10 (dd, $J = 1.05, 18.3$ Hz, 1H), 3.30 (m, 1H), 3.37 (m, 2H), 3.50 (m, 1H), 6.08 (q, $J = 7.2$ Hz, 1H), 7.24–7.36 (m, 5H). ^{13}C NMR (100 MHz, CDCl_3) δ 16.1, 33.4, 39.6, 49.3, 49.6, 50.1, 127.1, 127.3, 128.5, 139.3, 165.9.

ASSOCIATED CONTENT

Supporting Information

^1H NMR and ^{13}C NMR spectra of the two new compounds **11** and **12** and their respective CIFs. Additionally, it is included the ^1H NMR spectra of **10–16** in order to observe with precision the chemical shift of H_α . Geometries, electronic energies, ZPE and D3 correction of all minima calculated, and also molecular graphs showing bond critical points are included. This material is available free of charge via the Internet at <http://pubs.acs.org>.

AUTHOR INFORMATION

Corresponding Authors

*E-mail: julio.hernandez@correo.buap.mx

*E-mail: fernando.sartillo@correo.buap.mx

*E-mail: joel.teran@correo.buap.mx

Notes

The authors declare no competing financial interest.

ACKNOWLEDGMENTS

We gratefully acknowledge financial support from CONACyT (grant number: 179074) and Benemérita Universidad Autónoma de Puebla (BUAP-VIEP). J.S.-L. and L.F. thank CONACyT for graduate scholarships (grant numbers: 266627 and 104459, respectively).

REFERENCES

- (a) Sheiner, S. *Hydrogen Bonding: A Theoretical Perspective*; Oxford University Press: New York, 1997. (b) Jeffrey, G. A.; Saenger, W. *Hydrogen Bonding in Biological Structures*; Springer-Verlag: Berlin, 1991. (c) Donohue, J. In *Structural Chemistry and Molecular Biology*; Rich, A., Davidson, N., Eds.; W. H. Freeman: San Francisco, CA, 1968; pp 459–463.
- (2) (a) Steiner, T. *Angew. Chem., Int. Ed.* **2002**, *41*, 48–76. (b) Steiner, T. *J. Phys. Chem. A* **2000**, *104*, 433–435. (c) Desiraju, G. R.; Steiner, T. *The Weak Hydrogen Bond in Structural Chemistry and Biology*; Oxford University Press: Oxford, 1999. (d) Desiraju, G. R. *Science* **1997**, *278*, 404–405. (e) Desiraju, G. R. *Acc. Chem. Res.* **1996**, *29*, 441–449.

- (3) Representative publications: (a) Mottamalm, M.; Lazaridis, T. *Biochemistry* **2005**, *44*, 1607–1613. (b) Castellano, R. K. *Curr. Org. Chem.* **2004**, *8*, 845–865. (c) Yohannan, S.; Faham, S.; Yang, D.; Grosfeld, D.; Chamberlain, A. K.; Bowie, J. U. *J. Am. Chem. Soc.* **2004**, *126*, 2284–2285. (d) Chamberlain, A. K.; Bowie, J. U. *J. Mol. Biol.* **2002**, *322*, 497–503. (e) Vargas, R.; Garza, J.; Dixon, D. A.; Hay, B. P. *J. Am. Chem. Soc.* **2000**, *122*, 4750–4755. (f) Nagawa, Y.; Yamagaki, T.; Nakanishi, H. *Tetrahedron Lett.* **1998**, *39*, 1393–1396. (g) Seiler, P.; Weisman, R.; Glendening, E. D.; Weinhold, F.; Johnson, V. B.; Dumitz, J. D. *Angew. Chem., Int. Ed. Engl.* **1987**, *26*, 1175–1177.
- (4) (a) Parthasarathi, R.; Subramanian, V.; Sathyamurthy, N. *J. Phys. Chem. A* **2006**, *110*, 3349–3351. (b) Scheiner, S.; Kar, T.; Gu, Y. *J. Biol. Chem.* **2001**, *276*, 9832–9837.
- (5) (a) Corey, E. J.; Rohde, J. J. *Tetrahedron Lett.* **1997**, *38*, 37–40. (b) Corey, E. J.; Rohde, J. J.; Fischer, A.; Azimioara, M. D. *Tetrahedron Lett.* **1997**, *38*, 33–36.
- (6) Jones, C. R.; Baruah, P. K.; Thompson, A. L.; Scheiner, S.; Smith, M. D. *J. Am. Chem. Soc.* **2012**, *134*, 12064–12071.
- (7) (a) Rodríguez-Soria, V.; Sánchez, M.; Quintero, L.; Sartillo-Piscil, F. *Tetrahedron* **2004**, *60*, 10809–10815. This pyrrolidine was previously prepared by Orena and co-workers: (b) Cardillo, B.; Galeazzi, R.; Mobbili, G.; Orena, M.; Rossetti, M. *Heterocycles* **1994**, *38*, 2663–2676.
- (8) Juaristi, E.; Escalante, J.; León-Romo, J. L.; Reyes, A. *Tetrahedron: Asymmetry* **1998**, *9*, 715–740.
- (9) (a) Rodríguez-Soria, V.; Quintero, L.; Sartillo-Piscil, F. *Tetrahedron* **2008**, *64*, 2750–2754. (b) Rodríguez-Soria, V.; Quintero, L.; Sartillo-Piscil, F. *Tetrahedron Lett.* **2007**, *48*, 4305–4308.
- (10) (a) Sandoval-Lira, J.; Hernández-Pérez, J. M.; Sartillo-Piscil, F. *Tetrahedron Lett.* **2012**, *53*, 6689–6693. (b) Fuentes, L.; Quintero, L.; Cordero-Vargas, Eustaquio, C.; Terán, J. L.; Sartillo-Piscil, F. *Tetrahedron Lett.* **2011**, *52*, 3630–3632.
- (11) (a) Becke, A. D. *J. Chem. Phys.* **1993**, *98*, 1372. (b) Lee, C.; Yang, W.; Parr, R. G. *Phys. Rev. B* **1988**, *37*, 785.
- (12) Hehre, W. J.; Ditchfield, R.; Pople, J. A. *J. Chem. Phys.* **1972**, *56*, 2257.
- (13) London, F. Z. *Phys.* **1930**, *63*, 245–279.
- (14) Kruse, H.; Goerigk, L.; Grimme, S. *J. Org. Chem.* **2012**, *77*, 10824–10834.
- (15) Goerigk, L.; Reimers, J. R. *J. Chem. Theory Comput.* **2013**, *9*, 3240–3251.
- (16) Lodewyk, M. W.; Siebert, M. R.; Tantillo, D. J. *Chem. Rev.* **2012**, *112*, 1839–1862.
- (17) Keith, T. A. *AIMAll* (version 12.05.09); TK Gristmill Software: Overland Park, KS, 2012; aim.tkgristmill.com.
- (18) Frisch, M. J.; Trucks, G. W.; Schlegel, H. B.; Scuseria, G. E.; Robb, M. A.; Cheeseman, J. R.; Scalmani, G.; Barone, V.; Mennucci, B.; Petersson, G. A.; Nakatsuji, H.; Caricato, M.; Li, X.; Hratchian, H. P.; Izmaylov, A. F.; Bloino, J.; Zheng, G.; Sonnenberg, J. L.; Hada, M.; Ehara, M.; Toyota, K.; Fukuda, R.; Hasegawa, J.; Ishida, M.; Nakajima, T.; Honda, Y.; Kitao, O.; Nakai, H.; Vreven, T.; Montgomery, J. A., Jr.; Peralta, J. E.; Ogliaro, F.; Bearpark, M.; Heyd, J. J.; Brothers, E.; Kudin, K. N.; Staroverov, V. N.; Kobayashi, R.; Normand, J.; Raghavachari, K.; Rendell, A.; Burant, J. C.; Iyengar, S. S.; Tomasi, J.; Cossi, M.; Rega, N.; Millam, J. M.; Klene, M.; Knox, J. E.; Cross, J. B.; Bakken, V.; Adamo, C.; Jaramillo, J.; Gomperts, R.; Stratmann, R. E.; Yazyev, O.; Austin, A. J.; Cammi, R.; Pomelli, C.; Ochterski, J. W.; Martin, R. L.; Morokuma, K.; Zakrzewski, V. G.; Voth, G. A.; Salvador, P.; Dannenberg, J. J.; Dapprich, S.; Daniels, A. D.; Farkas, Ö.; Foresman, J. B.; Ortiz, J. V.; Cioslowski, J.; Fox, D. J. *Gaussian 09*, revision B.01; Gaussian, Inc.: Wallingford, CT, 2009.
- (19) Bader, R. F. W. *Atoms in Molecules, A Quantum Theory*; Oxford University Press: Oxford, 1990.
- (20) (a) Kemnitz, C. R.; Loewen, M. J. *J. Am. Chem. Soc.* **2007**, *129*, 2521–2528. (b) Mujika, J. I.; Matxain, J. M.; Eriksson, L. A.; Lopez, X. *Chem.—Eur. J.* **2006**, *12*, 7215–7224.
- (21) Fuentes, L.; Osorio, U.; Quintero, L.; Höpfl, H.; Vázquez-Cabrera, N.; Sartillo-Piscil, F. *J. Org. Chem.* **2012**, *77*, 5515–5524.
- (22) CCDC 1038283 (11). These data can be obtained free of charge from The Cambridge Crystallographic Data Centre via www.ccdc.cam.ac.uk/data_request/cif.
- (23) CCDC 1038284 (12). These data can be obtained free of charge from The Cambridge Crystallographic Data Centre via www.ccdc.cam.ac.uk/data_request/cif.
- (24) Zárate, A.; Orea, L.; Juárez, J. R.; Castro, A.; Mendoza, A.; Gnecco, D.; Terán, J. L. *Synth. Commun.* **2014**, *44*, 2838–2847.
- (25) Koch, U.; P. L. A. Popelier, P. L. A. *J. Phys. Chem.* **1995**, *99*, 9747–9754.
- (26) Aparicio, D. M.; Terán, J. L.; Roa, L. F.; Gnecco, D.; Juárez, J. R.; Orea, M. L.; Mendoza, A.; Flores-Alamo, M.; Micouin, L. *Synthesis* **2011**, *14*, 2310–2320.
- (27) (a) Fuentes, L.; Hernández-Juárez, M.; Terán, J. L.; Quintero, L.; Sartillo-Piscil, F. *Synlett.* **2013**, *24*, 878–882. (b) Juárez-Calderón, M.; Aparicio, D. M.; Gnecco, D.; Juárez, J. R.; Orea, L.; Mendoza, A.; Sartillo-Piscil, F.; del Olmo, E.; Terán, J. L. *Tetrahedron Lett.* **2013**, *54*, 2729–2732.
- (28) Allinger, N. L.; Hirsch, J. A.; Miller, M. A.; Tyminski, I. J. *J. Am. Chem. Soc.* **1968**, *90*, 5773–5780.
- (29) Witosinska, A.; Musielak, B.; Serda, P.; Owinska, M.; Rys, B. *J. Org. Chem.* **2012**, *77*, 9784–9794.
- (30) (a) Hobza, P.; Havlas, Z. *Chem. Rev.* **2000**, *100*, 4253–4264. (b) Joseph, J.; Jemmis, E. D. *J. Am. Chem. Soc.* **2007**, *129*, 4620–4632.
- (31) (a) Staszewska-Krajewska, O.; Bocian, W.; Maciejko, M.; Szczesnik, P.; Szymczak, K.; Chmielewski, M.; Furman, B. *Arkivok* **2014**, *iii*, 143–153. See also (b) Stewart, W. E.; Siddall, T. H. *Chem. Rev.* **1970**, *70*, 517–551.
- (32) Palillero, A.; Terán, J. L.; Gnecco, D.; Juárez, J. R.; Orea, M. L.; Castro, A. *Tetrahedron Lett.* **2009**, *50*, 4208–4211.